

Journal Pre-proof

Biotransformation of 2,4,6-Trinitrotoluene by *Pseudomonas* sp. TNT3 isolated from Deception Island, Antarctica

Ma. Ángeles Cabrera, Sebastián L. Márquez, Carolina P. Quezada, Manuel I. Osorio, Eduardo Castro-Nallar, Fernando D. González-Nilo, José M. Pérez-Donoso



PII: S0269-7491(19)32037-8

DOI: <https://doi.org/10.1016/j.envpol.2020.113922>

Reference: ENPO 113922

To appear in: *Environmental Pollution*

Received Date: 19 April 2019

Revised Date: 11 December 2019

Accepted Date: 5 January 2020

Please cite this article as: Cabrera, Ma.Á., Márquez, Sebastián.L., Quezada, C.P., Osorio, M.I., Castro-Nallar, E., González-Nilo, F.D., Pérez-Donoso, José.M., Biotransformation of 2,4,6-Trinitrotoluene by *Pseudomonas* sp. TNT3 isolated from Deception Island, Antarctica, *Environmental Pollution* (2020), doi: <https://doi.org/10.1016/j.envpol.2020.113922>.

This is a PDF file of an article that has undergone enhancements after acceptance, such as the addition of a cover page and metadata, and formatting for readability, but it is not yet the definitive version of record. This version will undergo additional copyediting, typesetting and review before it is published in its final form, but we are providing this version to give early visibility of the article. Please note that, during the production process, errors may be discovered which could affect the content, and all legal disclaimers that apply to the journal pertain.

© 2020 Published by Elsevier Ltd.

CRedit author statement

Ma. Ángeles Cabrera: Conceptualization, Methodology, Validation, Formal analysis, Investigation, Data Curation, Writing - Original Draft, Writing - Review & Editing, Visualization, Supervision, Project administration.

Sebastián L. Márquez: Conceptualization, Methodology, Software, Validation, Formal analysis, Data Curation, Writing - Original Draft, Writing - Review & Editing, Visualization.

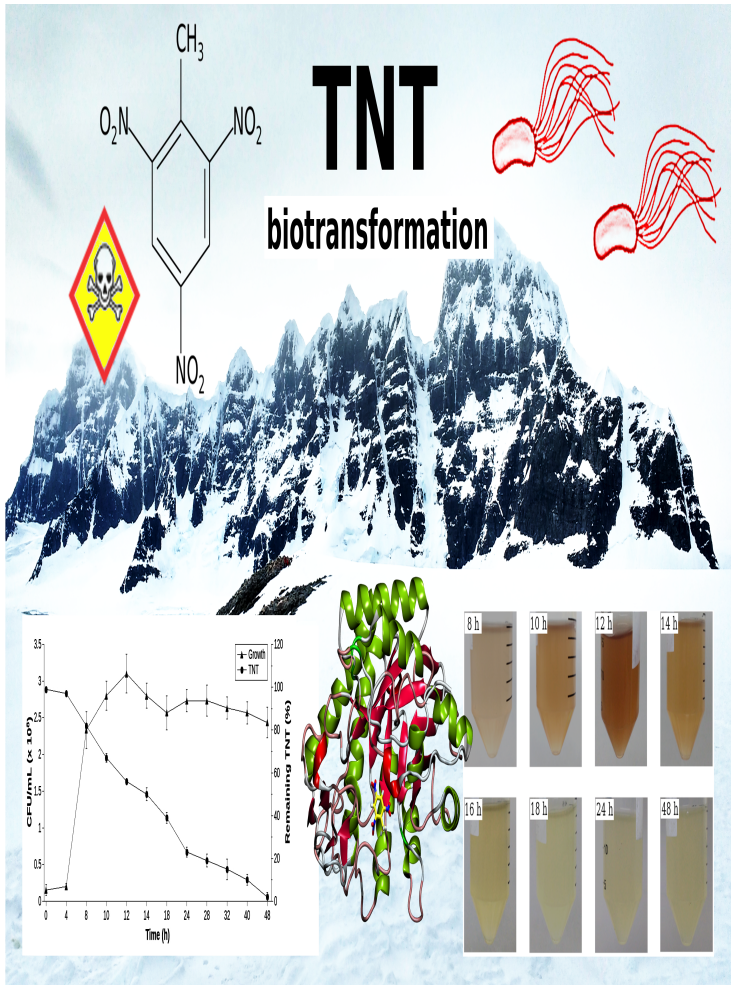
Carolina P. Quezada: Methodology, Investigation, Resources, Data Curation, Writing - Review & Editing, Visualization, Funding acquisition.

Manuel I. Osorio: Methodology, Software, Formal analysis, Data Curation, Writing - Original Draft, Visualization.

Eduardo Castro-Nallar: Resources, Writing - Review & Editing.

Fernando D. González-Nilo: Resources, Writing - Review & Editing.

José M. Pérez-Donoso: Conceptualization, Resources, Writing - Review & Editing, Supervision, Project administration, Funding acquisition.



1 **Biotransformation of 2,4,6-Trinitrotoluene by *Pseudomonas* sp. TNT3**

2 **isolated from Deception Island, Antarctica**

3
4 Ma. Ángeles Cabrera, Sebastián L. Márquez, Carolina P. Quezada, Manuel I. Osorio, Eduardo Castro-Nallar, Fernando D.
5 González-Nilo, and José M. Pérez-Donoso*

6
7 Center for Bioinformatics and Integrative Biology (CBIB), Faculty of Life Sciences, Universidad Andrés Bello, Av.
8 República 330, Santiago, Chile

9
10 Corresponding author: José M. Pérez-Donoso

11 E-mail: jose.perez@unab.cl

12 **Abstract**

13
14 2,4,6-Trinitrotoluene (TNT) is a nitroaromatic explosive, highly toxic and mutagenic for organisms. In this study,
15 we report for the first time the screening and isolation of TNT-degrading bacteria from Antarctic environmental samples
16 with potential use as bioremediation agents. Ten TNT-degrading bacterial strains were isolated from Deception Island.
17 Among them, *Pseudomonas* sp. TNT3 was selected as the best candidate since it showed the highest tolerance, growth, and
18 TNT biotransformation capabilities. Our results showed that TNT biotransformation involves the reduction of the nitro
19 groups. Additionally, *Pseudomonas* sp. TNT3 was capable of transforming 100 mg/L TNT within 48 h at 28°C, showing
20 higher biotransformation capability than *Pseudomonas putida* KT2440, a known TNT-degrading bacterium. Functional
21 annotation of *Pseudomonas* sp. TNT3 genome revealed a versatile set of molecular functions involved in xenobiotic
22 degradation pathways. Two putative xenobiotic reductases (XenA_TNT3 and XenB_TNT3) were identified by means of
23 homology searches and phylogenetic relationships. These enzymes were also characterized at molecular level using
24 homology modeling and molecular dynamics simulations. Both enzymes share different levels of sequence similarity with
25 other previously described TNT-degrading enzymes and with their closest potential homologues in databases.

26
27 **Capsulate:** First report of a TNT-degrading bacterium from Antarctica with potential use as bioremediation agent.

28 1. Introduction

29 2,4,6-Trinitrotoluene (TNT) is a nitroaromatic explosive widely used for military activities, building demolitions,
30 and mining explosions (Serrano-González et al. 2018). Massive TNT production, testing of munitions, and
31 decommissioning activities have generated large quantities of this compound as a waste product, contaminating soils and
32 groundwater around the world (Khan, Lee, and Park 2013). In addition, TNT is highly polluting and persistent in the
33 environment due to its symmetrical chemical structure, which hinders its degradation by microbial enzymes (Esteve-Núñez,
34 Caballero, and Ramos 2001). This is a relevant environmental problem considering the high toxicity of this compound and
35 its metabolites, which are carcinogenic and mutagenic for living organisms (Sabbioni et al. 2005; Won, DiSalvo, and Ng
36 1976). The exposure to this explosive has many other negative effects on human health, including skin irritation, cataracts,
37 anemia, and liver necrosis (EPA 2014). Therefore, the United States Environmental Protection Agency (US EPA) considers
38 its removal from the environment as a major priority (EPA 2014).

39 Nowadays, several physical/chemical methods are used to remove TNT from soil, such as incineration, detonation
40 or chemical oxidation. Unfortunately, these procedures are cost-intensive, ineffective, and can generate toxic by-products
41 (Ayoub et al. 2010; Singh, Kaur, and Singh 2012). Thus, there is an urgent need for new alternatives to remove TNT from
42 the environment. One advantageous approach is the use of microorganisms -or their enzymes- as bioremediation agents,
43 since they represent an environmentally friendly and low-cost alternative that can be carried out *in situ*. Regarding this
44 subject, TNT biodegradation activity has been reported in bacteria (*Pseudomonas*, *Bacillus*, *Achromobacter*, *Citrobacter*,
45 *Klebsiella*) and fungi (*Yarrowia*, *Irpex*, *Phanerochaete*) (Habineza et al. 2017; Jain et al. 2004; Kim and Song 2003; Kontro
46 et al. 2015; Serrano-González et al. 2018).

47 Under aerobic conditions, biological TNT degradation occurs by reductive metabolism. Two main classes of
48 enzymes are involved in this process: Type I Nitroreductases (group A, B1, and B2) and Old Yellow Enzymes (OYEs),
49 such as xenobiotic reductase A (XenA), xenobiotic reductase B (XenB), pentaerythritol tetranitrate reductase (PETNr), and
50 *N*-ethylmaleimide reductase (NEMr). Both nitroreductases and OYEs are NAD(P)H-dependent enzymes and use flavin
51 mononucleotide (FMN) as cofactor. Type I Nitroreductases reduce the nitro groups of TNT to hydroxylamino or amino
52 groups, producing different isomers of aminonitroaromatic compounds, such as hydroxylaminodinitrotoluenes (HADNTs),
53 aminodinitrotoluenes (ADNTs), diaminonitrotoluenes (DANTs), azo-, and azoxy- derivatives (Kim, Bennett, and Song
54 2002; Kim and Song 2003). On the other hand, OYEs mainly reduce nitro groups although some of them can also reduce
55 the TNT aromatic ring (Esteve-Núñez et al. 2001; Khan et al. 2013; Roldán et al. 2008). In the latter, the aromatic ring is
56 reduced to form mono- and dihydride-Meisenheimer complexes (adducts of aromatic nitrocompounds). It has been
57 proposed that this process produces nitrite ions and dinitrotoluenes (DNTs). However, it is still under discussion (Kim et al.

58 2002; Martin et al. 1997). Another mechanism indicates that Meisenheimer complexes and HADNTs can condense to form
59 secondary diarylamines and nitrite ions as the end-products (Wittich et al. 2008). The reduction of the aromatic ring is a
60 difficult process. Nevertheless, some OYEs capable to catalyze this reaction have been reported, e.g. PETNr from
61 *Enterobacter cloacae* PB2 (French, Nicklin, and Bruce 1998) and XenB from *Pseudomonas fluorescens* I-C (Pak et al.
62 2000).

63 Most of the TNT-degrading microorganisms have been isolated from TNT-contaminated sites (Chien et al. 2014;
64 Gumuscu and Tekinay 2013; Lee et al. 2009; Mercimek et al. 2013; Oh, Sarath, and Shea 2001). Nonetheless, to date, there
65 is no effective strategy for bioremediation of this compound, mainly due to the slow conversion rates, incomplete
66 biodegradation, and toxic effects on the microorganisms, among others (Berthe-Corti et al. 1998; Martin et al. 1997; Tam et
67 al. 2006). Therefore, we decided to search for TNT-degrading bacteria in an extreme environment, such as Antarctica. This
68 continent of unexplored genetic diversity represents an interesting source of microorganisms and enzymes with unknown -
69 and potentially useful- properties and applications (Cabrera and Blamey 2017; Gallardo et al. 2014; Gran-Scheuch et al.
70 2017; Márquez and Blamey 2019). Moreover, there is evidence that Antarctic microorganisms are capable to metabolize
71 different toxic compounds, although they have not been exposed to them before (Cabrera and Blamey 2017; Jung et al.
72 2013; Márquez and Blamey 2019).

73 In this study, we searched for TNT-degrading bacteria present in different sites of Antarctica in order to find
74 alternatives for bioremediation of TNT-contaminated soils out of this continent, particularly those contaminated by military
75 activities. TNT-degrading strains belonging to the genus *Pseudomonas* were isolated from Deception Island. One particular
76 isolate, named *Pseudomonas* sp. TNT3, was selected for further analyses because of its high capability to grow on TNT and
77 transform it. Genome analysis revealed that this strain possesses enzymes that participate in a variety of molecular
78 functions related to xenobiotic degradation. Additional analyses yielded evidence of the presence of two putative
79 xenobiotic reductases that we propose as potential candidates for the observed TNT transformation activity. Besides, these
80 enzymes share different levels of sequence similarity with other previously described TNT-degrading enzymes, including
81 their closest potential homologues in public databases.

82

83 **2. Materials and methods**

84 *2.1 Sampling and enrichment cultures*

85 Environmental soil samples were collected from Union Glacier, Antarctic Peninsula and the South Shetland
86 Islands in Antarctica during the 54th Antarctic Scientific Expedition (ECA) in 2018. Enrichment cultures were performed in
87 R2A medium (Reasoner and Geldreich 1985) at 21°C using constant agitation (180 rpm). Once bacterial growth was

88 observed, the microorganisms were transferred to R2A-TNT medium (half-diluted R2A medium containing 100 mg/L
89 TNT) and grown under the same conditions.

90

91 2.2 Isolation and identification of TNT-degrading microorganisms

92 After four serial transfers in liquid R2A-TNT medium ($OD_{600} > 0.2$), the cultures were transferred to agar plates of
93 the same medium (1.5% wt/vol) and single colonies were isolated. To identify the TNT-degrading microorganisms,
94 genomic DNA was extracted using the Wizard Genomic DNA Purification (Promega). Total DNA was used to amplify the
95 16S rRNA gene by PCR using universal bacterial primers (27F and 1525R) (Wawrik et al. 2005). Then, PCR products were
96 sequenced and compared to the Ribosomal Database Project (RDP) and the 16S Microbial Database of NCBI for
97 taxonomic identification. Subsequently, the MEGA7 software package (Kumar, Stecher, and Tamura 2016) was used to
98 infer a phylogenetic tree using the Neighbor-Joining method. Distances were computed using the maximum composite
99 likelihood model with a bootstrap analysis of 1000. *Escherichia coli* UMN026 was used as outgroup.

100

101 2.3 Growth of bacterial isolates on TNT

102 All isolates were grown in liquid half-diluted R2A medium containing 100 or 250 mg/L TNT, at 21°C for 6 days
103 using constant agitation. The bacterial growth was assessed by measuring the optical density at 600 nm (OD_{600}). Then, the
104 cultures were centrifuged at 14,000 x g for 10 min and the supernatant was recovered for the quantification of the
105 remaining TNT. The OD_{600} of controls (corresponding to uninoculated medium containing TNT and supernatants of each
106 culture) were considered.

107 The growth on TNT and its consumption (disappearance from the culture medium) by selected bacterial isolates
108 were evaluated on different liquid culture media at 28°C for 6 days under aerobic conditions. To assess the utilization of
109 TNT as carbon, nitrogen or carbon-nitrogen source, culture media were prepared as follows: C medium (TNT as sole
110 nitrogen source) consisted of modified saline M9 minimal medium (Cold Spring Harbor Protocols 2010) (without NH_4Cl
111 and containing 0.8% glucose as carbon source). N medium (TNT as sole carbon source) consisted of modified saline M9
112 medium (containing 0.05% NH_4Cl as nitrogen source). S medium (TNT as carbon and nitrogen source) consisted of
113 modified saline M9 medium (without NH_4Cl). CN medium consisted of half-diluted R2A medium (it contains low levels of
114 complex carbon and nitrogen sources). TNT was used at a concentration of 100 mg/L.

115 For the TNT consumption analysis, *Pseudomonas* sp. TNT3 was grown in R2A-TNT medium at 28°C using
116 agitation. Then, 1 mL-aliquots were taken from each culture for 48 h to assess bacterial growth by measuring the optical
117 density at 600 nm and by counting colony forming units (CFU) on plates (expressed as CFU/mL).

118 2.4 Quantification of TNT and nitrite

119 TNT concentration in bacterial cultures was determined as described before (Oh et al. 2000) (Figure S1). Briefly,
120 100 μL of culture supernatants were mixed with 900 μL of 50 mM Tris-HCl buffer (pH 7.0). Then, 160 μL of 1 M NaOH
121 were added and the reaction was incubated for 10 min at 21°C. The TNT concentration was determined
122 spectrophotometrically at 447 nm. Control experiments were carried out to measure the abiotic decomposition of TNT. All
123 assays were performed in triplicate.

124 Nitrite concentration in bacterial cultures was determined as described by Mercimek et al. (2015). Briefly, 200 μL
125 of culture supernatants were mixed with 50 μL of 1% sulfanilamide, 50 μL of 0.1% *N*-(1-naphthyl) ethylenediamine
126 dihydrochloride, and 700 μL of deionized water. The reaction mixture was incubated for 20 min at 21°C. Nitrite
127 concentration was determined at 540 nm. All assays were performed in triplicate.

129 2.5 TNT biotransformation by bacterial cells

130 For High-Performance Liquid Chromatography (HPLC) experiments, the same quantity of *Pseudomonas* sp.
131 TNT3 and *P. putida* KT2440 cells was incubated at 28°C for 48 h in R2A-TNT medium (100 mg/L TNT). For the
132 extraction of nitroaromatic compounds, the cultures were centrifuged at 14,000 $\times g$ for 10 min and the supernatant was
133 recovered. Then, NaCl (2.5 M final) was added to it. After dissolving, 1 volume of acetonitrile was added, followed by
134 vigorous agitation. The upper phase was extracted, filtered using polytetrafluoroethylene (PTFE) filters and placed in
135 HPLC sample vials. HPLC was performed using an Agilent Technologies 1260 Infinity II equipment with a UV detector at
136 254 nm. Chromatographic separation was performed by injecting a sample volume of 10 μL into a C18-RP column
137 (Sunshell C18, 2.6 μm) at 30°C. The mobile phase comprised of 21% (v/v) acetonitrile, 35% methanol, and 44% deionized
138 water. This phase was isocratically delivered to the column at a flow rate of 0.7 mL/min (Chien et al. 2014).

140 2.6 Tolerance to TNT

141 Tolerance to TNT was evaluated by culturing the same quantity of strains TNT3 and KT2440 cells in liquid half-
142 diluted R2A medium containing different concentrations of the compound (0, 100, 200, 300, 400, and 500 mg/L) for 48 h
143 at 28°C. Then, bacterial growth (OD_{600}) and TNT consumption were assessed. Control experiments were performed as
144 described previously. All experiments were carried out in triplicate.

148 2.7 *Statistical analysis*

149 To assess statistically significant differences between more than two groups of data, a 2-way analysis of variance
150 (ANOVA) was performed, followed by Tukey post hoc test for comparing each different group ($p < 0.05$). All statistical
151 analyses were performed using the GraphPad Prism v8.0 software.

152

153 2.8 *Genome sequencing and annotation*

154 Whole genome of TNT3 isolate was sequenced on an Illumina MiSeq platform using a 2 x 300 bp paired-end
155 sequencing protocol at the Center of Plant Biotechnology (Universidad Andrés Bello, Santiago, Chile). Raw reads were
156 filtered out using BBDuk (Bushnell 2015) to remove low quality reads, contaminant sequences and to trim-off poor quality
157 bases from both ends. Filtered reads were assembled *de novo* into contigs using SPAdes assembler (Bankevich et al. 2012).
158 Genome annotation was performed using PROKKA (Seemann 2014). Complementary genome-wide functional annotation
159 was computed using eggNOG-mapper (Huerta-Cepas et al. 2017) based on eggnog 4.5 database (Huerta-Cepas et al. 2016).
160 Additionally, all amino acid sequences were submitted to KEGG's BlastKOALA annotation server (Kanehisa, Sato, and
161 Morishima 2016) for KEGG ortholog ID assignment and mapping to KEGG pathways (KEGG Orthology).

162

163 2.9 *Search of TNT-degrading enzymes*

164 For the identification of potential TNT-degrading enzymes in the genome of the TNT3 isolate, homology searches
165 were performed using BLAST+ (Camacho et al. 2009) and HMMER's hmmscan tool (Eddy 2011) and the protein
166 translation of open reading frames (ORFs) predicted by PROKKA as queries. Searches were performed against a custom
167 database of 12 well-characterized Nitroreductases and Old Yellow Enzymes active towards TNT (Uniprot accessions:
168 P77258, P0ACY1, A0A0T9VMV0, Q5XW77, P17117, AAD18027, Q7B4Y3, Q56691, Q6DLR9, AAB38683,
169 AAF02538, AAF02539). For HMMER search, the database was converted into a Hidden Markov Model (HMM) profile by
170 performing a multiple sequence alignment with Clustal Omega (Sievers and Higgins 2014) and then using it as input for
171 HMMER's hmmbuild tool.

172

173 2.10 *Homology modeling and molecular dynamics*

174 To evaluate the theoretical affinity of the identified enzymes for the substrate TNT, homology models and
175 molecular dynamics simulations were carried out. Template searches for homology modelling were performed using
176 SWISSMODEL server (Waterhouse et al. 2018). The crystal structures with higher ranks according to the server quality
177 estimator (GMQE) were used as templates for model building. Homology modelling was performed by using the Prime's

178 homology model package (Jacobson et al. 2004) included in the Schrodinger suite. Molecular structures of TNT and FMN
179 were built with Gaussview (Dennington, Keith, and Millam 2009) and then optimized using the B3LYP/6-31G* DFT
180 method as implemented in Gaussian 16 (Frisch et al. 2016). Ligand atomic charges were calculated using Restrained
181 Electrostatic Potential (RESP) fits. Enzyme-ligand systems for simulation were prepared using the Protein Preparation
182 Wizard package available in the Schrodinger suite, considering protonation states of the ionizable residues at pH 7.0 as
183 determined by the H ++ server (Gordon et al. 2005) and electrical neutrality achieved by adding counterions. The enzyme-
184 ligand systems were immersed in solvation boxes of TIP3 water molecules (10 Å). All molecular dynamics simulations
185 were performed with the GPU-accelerated implementation of AMBER18 (Case et al. 2005; Lee et al. 2018), using the
186 ff14SB force field for proteins. Molecular dynamics simulation protocol is detailed in supplementary material (Protocol
187 S1). Enzyme-ligand affinities were estimated by using Molecular Mechanics with Generalized Born Surface Area
188 continuum solvation (MM/GBSA) method (Genheden and Ryde 2015) to calculate the free energy of binding (ΔG_{bind}), as
189 implemented in AMBER18. For free energy calculations, only the last 100 ns of each simulation were considered.

190

191 3. Results and discussion

192 3.1 Screening and isolation of TNT-degrading bacteria from Antarctica

193 A total of 33 enrichment cultures were performed from Antarctic sites (Figure S2 and Table S1). The selected sites
194 have different geological characteristics as described as follows: Union Glacier, a glacier with soil temperatures around -
195 4°C (Charles Peak, Rossman Cove, Elephant Head). Deception Island, a crater of a submarine volcano with high
196 geothermal activity. Antarctic Peninsula (O'Higgins Station) and different islands from the South Shetland archipelago
197 (King George, Greenwich, and Livingstone islands) with constant human activity. Bacterial growth was observed in all
198 enrichment cultures using R2A medium. Nevertheless, when mixed cultures -obtained from the enrichments- were grown
199 in R2A-TNT medium (half-diluted R2A medium containing 100 mg/L TNT), bacterial growth was observed only in two of
200 them, indicating that this kind of microorganisms are not ordinary inhabitants in this extreme environment. The two mixed
201 cultures that were able to grow in presence of TNT, named ID5 and ID6, were obtained from samples belonging to
202 Deception Island (Table S1). Subsequently, a total of 10 Antarctic TNT-degrading bacteria were isolated from the mixed
203 culture ID5 (TNT2, TNT7, TNT11, TNT14, and TNT18 isolates) and ID6 (TNT3, TNT4, TNT12, TNT15, and TNT19
204 isolates). These isolates are the first TNT-degrading microorganisms reported from Antarctica so far.

205 As TNT is a highly toxic compound, only those microorganisms capable of degrading or transforming it can thrive
206 in its presence. To date, the vast majority of TNT-degrading microorganisms have been isolated from TNT-contaminated
207 sites (Chien et al. 2014; Claus et al. 2007; Gumuscu and Tekinay 2013; Lee et al. 2009; Liang et al. 2017; Mercimek et al.

208 2013; Oh et al. 2001; Vorbeck et al. 1998). Nevertheless, in this study we discovered TNT-degrading bacteria from
209 Deception Island (the crater of a submarine volcano). As far as we know, this site is free from TNT contamination. As the
210 presence of aromatic compounds in volcanic emissions from other sources has been previously reported (Jordan 2003;
211 Pereira, Rostad, and Taylor 1980), we think that they could also be present in this site. In addition, they might have
212 chemical structures similar to TNT, which may explain the TNT-degrading activity of the bacteria isolated in this work.
213 This hypothesis is supported by recent reports of microorganisms capable to degrade nitriles and amines, isolated from the
214 same place (Cabrera and Blamey 2017; Márquez and Blamey 2019).

215

216 3.2 Growth and TNT consumption by the isolates

217 The 10 isolates obtained were able to grow in R2A-TNT medium under aerobic conditions. When the
218 microorganisms were cultivated at 21°C in half-diluted R2A medium containing 100 mg/L TNT, their growth was similar
219 (Figure 1a). However, when cultures were exposed to higher TNT concentration (250 mg/L), the growth was negatively
220 affected in most of the microorganisms, except TNT3, TNT12, and TNT19 isolates, whose growth was favored. The
221 highest growth was observed for the TNT3 isolate. Additionally, the capability of all isolates to consume TNT under these
222 conditions was evaluated. At 100 mg/L TNT (100 ppm) all microorganisms consumed ~90 ppm TNT, except the TNT15
223 isolate that showed the lowest consumption (Figure 1b). Nevertheless, at 250 mg/L TNT (250 ppm), the TNT3, TNT12,
224 and TNT19 isolates showed a higher TNT consumption than that observed at 100 mg/L. The TNT3 isolate showed the
225 highest TNT consumption (reaching 167 ppm TNT), whereas TNT15 isolate showed the lowest one (43 ppm).

226 As expected, the isolates that showed the highest growth at 250 mg/L TNT were those with better consumption
227 capability (TNT3, TNT12 and TNT19 isolates). These results suggest that these isolates might use this toxic compound as
228 an energy source. Indeed, depending on the degree of structural analogy between natural substrates and xenobiotics, the
229 enzymes that degrade the former could also degrade the latter (Rieger et al. 2002). Consequently, microorganisms (and/or
230 their enzymes) from pristine sites could degrade xenobiotics even if they have not been previously exposed to these
231 compounds (Cabrera and Blamey 2017; Giudice et al. 2010; Khan et al. 2014; Kitagawa et al. 2002; Márquez and Blamey
232 2019; Tralau et al. 2011). Due to the different growth and TNT consumption showed by TNT3, TNT11, and TNT19
233 isolates (TNT3 > TNT19 > TNT11), they were selected for further analyses.

234

235 3.3 Phylogenetic identification of the isolates

236 According to RDP and BLAST analyses of the 16S rRNA gene sequences, all the TNT-degrading isolates from
237 Antarctica belong to the genus *Pseudomonas*. The isolates are closely related to *P. marginalis* (TNT2, TNT7, TNT18

238 isolates), *P. brenneri* (TNT4 isolate), *P. migulae* (TNT12 isolate), *P. extremaustralis* (TNT14 isolate), and *P. trivialis*
239 (TNT15 isolate). On the other hand, phylogenetic analysis revealed that TNT3, TNT11, and TNT19 isolates are closer to *P.*
240 *fluorescens* strain CCM 2115 (96% identity), *P. veronii* strain CIP 104663 (98% identity), and *P. migulae* strain CIP
241 105470 (98% identity), respectively (Figure 2). Based on these results, the three isolates were renamed as *Pseudomonas* sp.
242 TNT3, *Pseudomonas* sp. TNT11, and *Pseudomonas* sp. TNT19. Although these microorganisms belong to a common
243 TNT-degrading bacterial genus, namely *P. putida* (Caballero et al. 2005; Van Dillewijn et al. 2008; Fernández et al. 2009),
244 *P. aeruginosa* (Mercimek et al. 2015; Oh et al. 2001), *P. pseudoalcaligenes* (Fiorella and Spain 1997), and *P. fluorescens*
245 (Pak et al. 2000), there are no TNT-degrading Antarctic *Pseudomonas* strains described so far.

246

247 3.4 Growth and TNT consumption by selected isolates in different media

248 To evaluate the use of TNT as carbon and/or nitrogen source, the strains TNT3, TNT11, and TNT19 were grown
249 in different media at 21°C (data not shown) and 28°C, being the latter the optimal temperature for growth and TNT
250 consumption. Therefore, at 28°C, the highest growth of the three isolates was in CN medium containing 100 mg/L TNT,
251 especially in the case of strain TNT3 (Figure 3a). Additionally, this growth was higher than that observed in the same
252 medium without TNT. No growth was observed for strains TNT11 and TNT19 in the other media (C, N, and S). However,
253 strain TNT3 showed a slight growth. All these isolates showed the highest TNT consumption in CN medium, especially
254 TNT3 that depleted 100% of the TNT (Figure 3b). Strains TNT11 and TNT19 showed a slight TNT consumption (<15%)
255 in the rest of the media, whereas strain TNT3 was capable to consume up to ~60% of the TNT.

256 In conclusion, the three bacteria tested require a culture medium containing low levels of an exogenous carbon and
257 nitrogen source to grow and consume TNT optimally, as reported by other studies (Liang et al. 2017; Muter et al. 2012; Oh
258 et al. 2003). These nutrients may provide energy and reducing equivalents (i.e. NAD(P)H), which are used for the increase
259 in biomass and the reduction of the TNT nitro groups (Rieger et al. 2002; Roldán et al. 2008).

260

261 3.5 TNT biotransformation

262 As mentioned above, *Pseudomonas* sp. TNT3 was capable of growing in CN medium containing 100 mg/L TNT.
263 The maximum bacterial growth in this medium was observed after 12 h of incubation (Figure 4a and S3). In contrast, TNT
264 consumption was initiated during early exponential phase, reaching 46% of the consumption at the end of this phase (12 h)
265 and 100% after 48 h. The decrease in CFUs of *Pseudomonas* sp. TNT3 after 12 h of incubation could be due to the toxicity
266 of some TNT metabolites accumulated in the medium (discussed below). The concentration of nitrite increased
267 significantly from 14 h to 48 h of incubation, reaching 8.9 µM (Figure 4b). This concentration is in agreement with other

268 studies (Mercimek et al. 2013, 2015; Oh et al. 2003). However, unlike what was reported in those works, the concentration
269 of nitrite did not increase during the exponential phase but rather in stationary phase. These results suggest that strain TNT3
270 might be using nitrite as nitrogen source (either directly or indirectly) during its growth. Then, during the stationary phase,
271 TNT3 cells may be using less nitrite and consequently it begins to accumulate in the medium.

272 Interestingly, a light orange color was observed in the culture medium when TNT3 cultures started to grow, which
273 turned gradually into a dark brownish-red color after incubating for 12 h (Figure 4c). Then, the culture medium turned into
274 a yellow color, which remained from 18 h of incubation until the end of the growth curve. These color changes has been
275 reported for TNT derivatives, such as oxidized dead-end metabolites and hydride-Meisenheimer complex (brownish-red)
276 (Vorbeck et al. 1998; Wittich et al. 2008), nitro-reduction products (orange-yellow) (Thijs et al. 2018), and HADNTs,
277 ADNTs, DANTs or dihydride-Meisenheimer complex (yellow) (Kim and Song 2003; Thijs et al. 2018; Vorbeck et al.
278 1998).

279 The TNT biotransformation by *Pseudomonas* sp. TNT3 was confirmed by HPLC. Under the conditions tested,
280 TNT consumption reached 50% after 12 h of incubation at 28°C (Figure 5c). In addition, an unknown metabolite and a
281 small amount of 2-amino-4,6-dinitrotoluene (2-A-4,6-DNT) were produced. After 48 h of incubation, TNT consumption
282 reached 85% (Figure 5e), the remaining amount of the unknown metabolite decreased and 2-A-4,6-DNT increased 7-fold.
283 The latter might negatively affect the viability of TNT3 cells during the stationary phase (Figure 4a). Indeed, it has been
284 reported that 2-A-4,6-DNT is not degraded further and could be as toxic as TNT itself (Eyers, Stenuit, and Agathos 2008).
285 On the other hand, this compound is an intermediate metabolite when the reduction of TNT nitro groups occurs in bacteria
286 (Esteve-Núñez et al. 2001; Maksimova, Maksimov, and Demakov 2018; Serrano-González et al. 2018). Therefore, its
287 presence indicates that *Pseudomonas* sp. TNT3 is capable of carrying out this pathway. Regarding DNTs, no evidence of
288 the presence of 2,4-dinitrotoluene (2,4-DNT) or 2,6-dinitrotoluene (2,6-DNT) was obtained (Figure 5c and 5e).

289 The TNT biotransformation by strain TNT3 was compared to that of *P. putida* KT2440. The latter is a model
290 bacterium for soil bioremediation, since it has a highly versatile metabolism. It is the best characterized TNT-degrading
291 *Pseudomonas* strain and possesses nitroreductases and OYEs enzymes (Fernández et al. 2009). At 12 h of incubation, strain
292 TNT3 transformed 50% TNT, while strain KT2440 was able to transform only 5%. Interestingly, strain KT2440 also
293 produced a very small amount of the same unknown metabolite at the same time (Figure 5d). After 48 h, this strain
294 transformed only 25% of TNT and produced an almost undetectable amount of 2-A-4,6-DNT (Figure 5f). Therefore,
295 *Pseudomonas* sp. TNT3 was able to transform TNT faster than *P. putida* KT2440 under the conditions tested. Like strain
296 TNT3, no evidence of the presence of DNTs in strain KT2440 supernatants was obtained.

297

298

299

300 3.6 Tolerance to TNT

301 The growth and TNT transformation by strain TNT3 increased significantly from 0 to 300 mg/L TNT (Figure 6a
302 and 6b, Table S2), reaching its maximum at this concentration. Then, they decreased quickly from 400 to 500 mg/L TNT.
303 The highest growth and TNT consumption at 300 mg/L TNT suggests that the bacterium could use TNT as a nutrient to
304 proliferate efficiently. This result agrees with the aerobic TNT metabolism in bacteria, because the denitration pathway
305 produces nitrite and toluene through a series of intermediates. Toluene could be used as carbon and energy source since it
306 can be incorporated into the TCA cycle, whereas nitrite could be used as nitrogen source by its reduction to ammonium,
307 which is assimilated via the GS-GOGAT pathway (Esteve-Núñez et al. 2001; Serrano-González et al. 2018; Stenuit and
308 Agathos 2010).

309 The growth and TNT consumption of the strain TNT3 were compared to those of strain KT2440. The latter
310 showed just a slight increase in its growth in presence of TNT (half of that observed in strain TNT3) and low TNT
311 consumption under the same conditions (Figure 6a and 6b, Table S2). In fact, strain TNT3 transformed more TNT than
312 strain KT2440 at all concentrations of this compound, particularly at 300 mg/L, where the former transformed 191 ppm and
313 the latter 75 ppm. Therefore, under these conditions *Pseudomonas* sp. TNT3 was capable to transform 2.5-fold more TNT
314 than *P. putida* KT2440. Interestingly, at 100-300 mg/L TNT, the growth of strain KT2440 was not improved by the
315 addition of the compound, as observed with strain TNT3. This result reinforces the novelty and metabolic advantages of
316 this Antarctic isolate in terms of TNT metabolism. The remarkable TNT-degrading behavior of strain TNT3 and its
317 differences in comparison to strain KT2440 suggest that the former might possess alternative metabolic routes, enzymes
318 with improved characteristics or maybe a different number of them that might favor TNT metabolism. Based on this, we
319 decided to predict the functional metabolic potential of strain TNT3 through genome analysis and mining for enzymes
320 involved in xenobiotic-degradation pathways.

321

322 3.7 Search of TNT-degrading enzymes and functional annotation

323 As one of our goals was to identify the enzymes potentially responsible for the TNT-degrading activity of the
324 *Pseudomonas* sp. TNT3, we performed a bioinformatic analysis of its genome sequence. Aiming to this, a draft genome
325 assembly for strain TNT3 was constructed using SPAdes assembler. The resulting assembled genome consisted of 252
326 contigs with an N50 of 81 kb. The obtained genome size (6.5 Mb) is consistent with the average genome size of different
327 species from the genus *Pseudomonas*, according to the available genomic data in the “*Pseudomonas* Genome Database”

328 (Winsor et al. 2009). Genome annotation with PROKKA revealed the presence of 5,903 coding sequences (CDSs), which
329 is also in good agreement with the number of coding sequences reported for other *Pseudomonas*, particularly for members
330 of the *P. fluorescens* species (Kahlon 2016).

331 From a total of 186 CDS annotated by PROKKA as “reductases”, 62 corresponded to “oxidoreductases”, which is
332 the group of enzymes where we focused our search. Nevertheless, as many reported TNT-degrading enzymes have similar
333 amino acid sequences (Toogood, Gardiner, and Scrutton 2010; Williams et al. 2004) and there is no clear consensus about
334 how to differentiate nitroreductases from OYEs (i.e. look for the presence of key residues or motifs), discriminating among
335 them based only on automatic annotations is usually not reliable. Thus, although several sequences were annotated by
336 PROKKA as “NAD(P)H-dependent-” or “FMN-” oxidoreductases (which are generic names for many nitroreductases and
337 OYEs), a deeper analysis was needed to identify those that might be responsible for TNT-degrading activity. As a first
338 approach, we performed an analysis based on homology searches with BLASTp and HMMER against a custom TNT-
339 degrading enzymes database (see materials and methods). BLASTp homology results only yielded significant matches for
340 two coding sequences: CDS_02682 and CDS_03039, which matched to XenA (accession AAF02538) from *P. putida*
341 (46.6% identity) and XenB (accession AAF02539) from *P. fluorescens* (91.6% identity), respectively. Remote homologues
342 search using HMMER yielded 7 significant matches to the hmm profile database, two of which coincided with the previous
343 BLAST results as shown in Table S3. This allowed us to limit the number of sequences to consider in the following
344 analysis. The 7 identified sequences were initially annotated by PROKKA as follows: *N*-ethylmaleimide reductase
345 (CDS_03039), NADPH dehydrogenase (CDS_02682), NADH oxidase (CDS_03801), Putative NAD(P)H nitroreductase
346 YdjA (CDS_01069), 5,6-dimethylbenzimidazole synthase (CDS_00209), putative *N*-methylproline demethylase
347 (CDS_00327), and 2,4-dienoyl-CoA reductase A (CDS_01856) (Table 1).

348 To gather functional evidence of these sequences, we performed a complementary functional annotation with
349 BlastKOALA and egg-NOG servers for all the coding sequences of the strain TNT3. According to the results obtained
350 using BlastKOALA, 3,108 CDSs (52.7%) were assigned to KO IDs, which means that each of them was classified into an
351 ortholog group of the database. Of these, 162 CDSs belonging to 101 different groups of orthologs, were mapped into 17
352 KEGG pathways of the “Xenobiotic biodegradation and metabolism” category (Figure 7). Curiously, none of the sequences
353 identified by homology searches was assigned to a KO ID nor mapped to any of the xenobiotic degradation pathways, as
354 we would have expected. For comparison purposes, we also annotated the genome of *P. putida* KT2440 using KEGG’s
355 BlastKOALA and compared the total counts of proteins assigned to an ortholog group (KO ID) of the “Xenobiotic
356 biodegradation and metabolism” set of pathways to that determined in strain TNT3. As a result, we found that a smaller
357 number of ortholog groups were present in strain KT2440 than in strain TNT3 (96 vs 101 KOs, respectively) and also a

358 smaller number of proteins (143 vs 162, respectively). Moreover, it is interesting to note that in 9 of the 19 pathways shown
359 in Figure 7 (degradation of polycyclic aromatic hydrocarbon, caprolactams, atrazine, styrene, toluene, chlorocyclohexane
360 and chlorobenzene, chloroalkane and chloroalkene, fluorobenzoate, and aminobenzoate) a greater number of proteins was
361 assigned to strain TNT3 than strain KT2440. This indicates that more molecular functions are present in the former and
362 suggests a likely greater metabolic potential to degrade xenobiotics.

363 Unlike the results obtained with BlastKOALA, 4 out of the 7 sequences identified by homology were indeed
364 assigned to a KO ID by functional annotation with egg-NOG server (Table 1). As a result, the sequences annotated with
365 PROKKA as “*N*-ethylmaleimide reductase” (CDS_03039) and “NADPH dehydrogenase” (CDS_02682) of *Pseudomonas*
366 sp. TNT3 were predicted to have orthologous relationships with the xenobiotic reductases XenB and XenA of *P.*
367 *fluorescens* (strains WH6 and Pf-5, respectively). Interestingly, the orthology number K10680 was assigned to the sequence
368 CDS_03039, which according to KEGG is a part of the “Nitrotoluene degradation” pathway (ko00633). These results
369 support the orthology evidence about xenobiotic degradation activity of this putative XenB of strain TNT3. Hence, all the
370 evidence points to “*N*-ethylmaleimide reductase” of strain TNT3 could be a XenB-like enzyme involved in TNT
371 metabolism.

372 Although the remaining sequences were not assigned to any KO IDs linked to biodegradation of xenobiotics, this
373 does not necessarily mean that they do not participate in it, especially considering that many enzymes and pathways
374 involved in biodegradation have not yet been characterized. Therefore, as not enough functional information is available for
375 them, we cannot discard their potential participation in xenobiotic degradation routes and we will continue to investigate
376 them in further works.

377

378 3.8 Homology modelling and molecular dynamics simulations

379 To gain more insights on the possible role of the two putative xenobiotic reductases found, we performed 3D
380 structure predictions using the template search function of SWISS-MODEL. As a result, the server revealed that “*N*-
381 ethylmaleimide reductase” (CDS_03039) shares high identity (86%) with the crystal structure of a XenB from
382 *Pseudomonas putida* (pdb ID: 4AB4), which was co-crystallized together with TNT to study the structural determinants for
383 aromatic ring reduction of these group of enzymes (not published). For “NADPH dehydrogenase” (CDS_02682), the
384 structural prediction results included different enzymes annotated as “chromate reductases” and “xenobiotic reductases A”,
385 all of them with identities below 56%, being the “chromate reductase” 5NUX from *Thermus scotodocus* SA-01 the one
386 with higher identity to CDS_02682 (56%). The similarity of this putative enzyme to chromate reductases is not surprising
387 since it has been reported that several bacterial nitroreductases also show chromate reductase activity (Ackerley et al. 2004;

388 Kwak, Lee, and Kim 2003). Since homology and functional/structural evidence points to “*N*-ethylmaleimide reductase”
389 and “NADPH dehydrogenase” as the candidates most likely to have TNT-degrading activity, they were renamed as
390 XenB_TNT3 and XenA_TNT3 for the following analysis, respectively.

391 We built homology models and then performed molecular dynamics simulations for both enzymes in complex
392 with TNT and the cofactor FMN. Homology models for XenA_TNT3 and XenB_TNT3 were built using 5NUX and 4AB4
393 as templates, respectively. The QMEAN score for the resulting models was over 0.6 and the Ramachandran plots showed
394 that most of the residues were positioned in favorable regions (Figure S4), which validates the good quality of them. Thus,
395 added to the high coverage (94% for XenA_TNT3 and 100% for XenB_TNT3) and identity (45% for XenA_TNT3 and
396 91% for XenB_TNT3) between the sequences and the templates used, allowed us to obtain good 3D representations for the
397 putative reductases found in *Pseudomonas* sp. TNT3.

398 Molecular dynamics simulations were carried out using the built models, as indicated in material and methods. As
399 a result, it was observed that in both systems the enzyme-ligand complex behaves in a similar way, maintaining the TNT
400 substrate near the cofactor (FMN) in the active site throughout the 300 ns of simulation. The conformations adopted by the
401 substrate in the active sites of XenA_TNT3 and XenB_TNT3 are shown in Figure 8a and 8b, respectively. As observed in
402 the figure, the TNT ligand was kept at a short distance from the catalytic site, which is consistent with the calculated free
403 energies of binding ($\Delta G_{\text{bind}} = -27.0$ kcal/mol for XenA_TNT3 and $\Delta G_{\text{bind}} = -30.5$ kcal/mol for XenB_TNT3), showing a high
404 and similar affinity of the enzymes for this substrate. In addition, the root-mean-square deviation of atomic positions
405 (RMSD) for the C α backbones of both models was less than 2 Å after 300 ns of dynamics (Figure S5), which confirms their
406 good stability.

407 Altogether, our *in silico* analysis shows the potential of XenA_TNT3 and XenB_TNT3 from *Pseudomonas* sp.
408 TNT3 as new enzymes than those reported. These results also indicate that XenB_TNT3 is likely to be a XenB enzyme. We
409 are currently performing experiments to specifically determine the role of these enzymes in TNT metabolism and also the
410 participation of the genes involved.

411

412 4. Conclusions

413 The experimental results and theoretical evidence presented in this work validate the exploration of extreme
414 environments as Antarctica to discover microorganisms with novel metabolic capacities such as xenobiotic degradation. In
415 particular, the Antarctic bacterium *Pseudomonas* sp. TNT3 is a promising strain for application in TNT bioremediation
416 since it possesses a great number of molecular functions and enzymes related to xenobiotic degradation. In fact, the
417 genomics and structural analyses revealed the presence of at least two enzymes that could be involved in TNT

418 transformation: XenA_TNT3 and XenB_TNT3. However, to further understand and evaluate the potential for
419 bioremediation of *Pseudomonas* sp. TNT3, more exhaustive studies, both theoretical and experimental, are required to
420 identify structural differences that allow understanding the physiological importance of these enzymes or others involved.

421

422 **Author contributions**

423 MAC and JMPD conceived and designed the manuscript and experiments. MAC performed all the experiments, except for
424 the preparation of samples for HPLC (performed by CPQ). MAC, SLM, and MIO analyzed the data. MAC, SLM, CPQ,
425 and JMPD wrote the paper. MAC, SLM, CPQ, MIO, ECN, FGN, and JMPD reviewed the paper.

426

427 **Declarations of interest**

428 None.

429

430 **Funding**

431 This work was supported by Erika Elcira Donoso López; RDECOM US Army [W911NF-17-2-0156]; FONDECYT
432 [1151255] (JMPD) and [3170718] (CPQ); INACH [RT_25-16 and FP_02-17] (Instituto Antártico Chileno, ECA54).

433

434 **Acknowledgments**

435 Authors acknowledge Dr. Carolina P. Quezada for facilitating the soil samples from Deception Island, Dr. Ignacio Poblete-
436 Castro for facilitating *P. putida* strain KT2440 and also the Chilean Army for their constant support and help with the TNT
437 work, particularly Mr. Martín Inzunza and the CIMI (Comando de Industria Militar e Ingeniería del Ejército de Chile).
438 ECN would like to thank Universidad Andrés Bello's high-performance computing cluster, Dylan, for providing data
439 storage, support, and computing power for genomic analyses.

440

441 **Supplementary data**

442 Supplementary information is shown in supporting material.

443

444 **References**

445 Ackerley, D. F., C. F. Gonzalez, M. Keyhan, R. Blake, and A. Matin. 2004. "Mechanism of Chromate
446 Reduction by the *Escherichia Coli* Protein, NfsA, and the Role of Different Chromate Reductases in
447 Minimizing Oxidative Stress during Chromate Reduction." *Environmental Microbiology* 6(8):851–60.

- 448 Ayoub, Kaidar, Eric D. van Hullebusch, Michel Cassir, and Alain Bermond. 2010. "Application of Advanced
449 Oxidation Processes for TNT Removal: A Review." *Journal of Hazardous Materials* 178(1–3):10–28.
- 450 Bankevich, Anton, Sergey Nurk, Dmitry Antipov, Alexey A. Gurevich, Mikhail Dvorkin, Alexander S.
451 Kulikov, Valery M. Lesin, Sergey I. Nikolenko, Son Pham, Andrey D. Prjibelski, Alexey V Pyskin,
452 Alexander V Sirotkin, Nikolay Vyahhi, Glenn Tesler, Max A. Alekseyev, and Pavel A. Pevzner. 2012.
453 "SPAdes: A New Genome Assembly Algorithm and Its Applications to Single-Cell Sequencing."
454 *Journal of Computational Biology*.
- 455 Berthe-Corti, L., H. Jacobi, S. Kleihauer, and I. Witte. 1998. "Cytotoxicity and Mutagenicity of a 2,4,6-
456 Trinitrotoluene (TNT) and Hexogen Contaminated Soil in *S. Typhimurium* and Mammalian Cells."
457 *Chemosphere* 37(2):209–18.
- 458 Bushnell, Brian. 2015. "BBMap (Version 37.75) [Software]." Available at
459 <https://Sourceforge.Net/Projects/Bbmap/>.
- 460 Caballero, Antonio, Juan J. Lázaro, Juan L. Ramos, and Abraham Esteve-Núñez. 2005. "PnrA, a New
461 Nitroreductase-Family Enzyme in the TNT-Degrading Strain *Pseudomonas Putida* JLR11."
462 *Environmental Microbiology* 7(8):1211–19.
- 463 Cabrera, Ma Ángeles and Jenny M. Blamey. 2017. "Cloning, Overexpression, and Characterization of a
464 Thermostable Nitrilase from an Antarctic *Pyrococcus* Sp." *Extremophiles* 21(5):861–69.
- 465 Camacho, Christiam, George Coulouris, Vahram Avagyan, Ning Ma, Jason Papadopoulos, Kevin Bealer, and
466 Thomas L. Madden. 2009. "BLAST+: Architecture and Applications." *BMC Bioinformatics*.
- 467 Case, David A., Thomas E. Cheatham, Tom Darden, Holger Gohlke, Ray Luo, Kenneth M. Merz, Alexey
468 Onufriev, Carlos Simmerling, Bing Wang, and Robert J. Woods. 2005. "The Amber Biomolecular
469 Simulation Programs." *Journal of Computational Chemistry*.
- 470 Chien, Chih Ching, Chih Ming Kao, De Yu Chen, Ssu Ching Chen, and Chien Cheng Chen. 2014.
471 "Biotransformation of Trinitrotoluene (TNT) by *Pseudomonas* Spp. Isolated from a TNT-Contaminated
472 Environment." *Environmental Toxicology and Chemistry* 33(5):1059–63.
- 473 Claus, H., T. Bausinger, I. Lehmler, N. Perret, G. Fels, U. Dehner, J. Preuß, and H. König. 2007.
474 "Transformation of 2,4,6-Trinitrotoluene (TNT) by *Raoultella Terrigena*." *Biodegradation* 18(1):27–
475 35.
- 476 Cold Spring Harbor Protocols. 2010. "M9 Minimal Medium (Standard)." P. pdb.rec12295 in *Cold Spring*
477 *Harbor Protocols*. Vol. 2010.

- 478 Dennington, Roy, Todd Keith, and John Millam. 2009. "GaussView, Version 5." *Semichem Inc.*, Shawnee
479 *Mission, KS.*
- 480 Van Dillewijn, Pieter, Rolf Michael Wittich, Antonio Caballero, and Juan Luis Ramos. 2008.
481 "Subfunctionality of Hydride Transferases of the Old Yellow Enzyme Family of Flavoproteins of
482 *Pseudomonas Putida.*" *Applied and Environmental Microbiology* 74(21):6703–8.
- 483 Eddy, Sean R. 2011. "Accelerated Profile HMM Searches." *PLoS Computational Biology*.
- 484 EPA. 2014. *Priority Pollutant List.* United States Environmental Protection Agency.
- 485 Esteve-Núñez, A., A. Caballero, and Juan L. Ramos. 2001. "Biological Degradation of 2,4,6-Trinitrotoluene."
486 *Microbiological and Molecular Biology Reviews* 65(3):335–52.
- 487 Fernández, Matilde, Estrella Duque, Paloma Pizarro-Tobías, Pieter van Dillewijn, Rolf Michael Wittich, and
488 Juan L. Ramos. 2009. "Microbial Responses to Xenobiotic Compounds. Identification of Genes That
489 Allow *Pseudomonas Putida* KT2440 to Cope with 2,4,6-Trinitrotoluene." *Microbial Biotechnology*
490 2(2):287–94.
- 491 Fiorella, PD and JC Spain. 1997. "Transformation of 2,4,6-Trinitrotoluene by *Pseudomonas*
492 *Pseudoalcaligenes* JS52." *Applied and Environmental Microbiology* 63(5):2007–15.
- 493 French, C. E., S. Nicklin, and Neil C. Bruce. 1998. "Aerobic Degradation of 2,4,6-Trinitrotoluene by
494 *Enterobacter Cloacae* PB2 and by Pentaerythritol Tetranitrate Reductase." *Applied and Environmental*
495 *Microbiology* 64(8):2864–68.
- 496 Frisch, M. J., G. W. Trucks, H. E. Schlegel, G. E. Scuseria, M. A. Robb, J. R. Cheeseman, G. Scalmani, V.
497 Barone, G. A. Petersson, Farkas, O., J. B. Foresman, and J. D. Fox. 2016. "Gaussian 16." *Gaussian,*
498 *Inc., Wallingford CT,.*
- 499 Gallardo, C., J. P. Monrás, D. O. Plaza, B. Collao, L. A. Saona, V. Durán-Toro, F. A. Venegas, C. Soto, G.
500 Ulloa, C. C. Vásquez, D. Bravo, and J. M. Pérez-Donoso. 2014. "Low-Temperature Biosynthesis of
501 Fluorescent Semiconductor Nanoparticles (CdS) by Oxidative Stress Resistant Antarctic Bacteria."
502 *Journal of Biotechnology* 187.
- 503 Genheden, Samuel and Ulf Ryde. 2015. "The MM/PBSA and MM/GBSA Methods to Estimate Ligand-
504 Binding Affinities." *Expert Opinion on Drug Discovery*.
- 505 Giudice, AL, V. Bruni, M. Domenico, and L. Michaud. 2010. "Psychrophiles - Cold-Adapted Hydrocarbon-
506 Degrading Microorganisms." Pp. 1897–1921 in *Handbook of Hydrocarbon and Lipid Microbiology,*
507 edited by Timmis K.N. Springer, Berlin, Heidelberg.

- 508 Gordon, John C., Jonathan B. Myers, Timothy Folta, Valia Shoja, Lenwood S. Heath, and Alexey Onufriev.
509 2005. "H++: A Server for Estimating PKas and Adding Missing Hydrogens to Macromolecules."
510 *Nucleic Acids Research*.
- 511 Gran-Scheuch, Alejandro, Edwar Fuentes, Denisse M. Bravo, Juan Cristobal Jiménez, and José M. Pérez-
512 Donoso. 2017. "Isolation and Characterization of Phenanthrene Degrading Bacteria from Diesel Fuel-
513 Contaminated Antarctic Soils." *Frontiers in Microbiology* 8:1634.
- 514 Gumuscu, Burcu and Turgay Tekinay. 2013. "Effective Biodegradation of 2,4,6-Trinitrotoluene Using a
515 Novel Bacterial Strain Isolated from TNT-Contaminated Soil." *International Biodeterioration and*
516 *Biodegradation* 85:35–41.
- 517 Habineza, Alphonse, Jun Zhai, Tianpeng Mai, Daniel Mmereki, and Theoneste Ntakirutimana. 2017.
518 "Biodegradation of 2, 4, 6-Trinitrotoluene (TNT) in Contaminated Soil and Microbial Remediation
519 Options for Treatment." *Periodica Polytechnica Chemical Engineering* 61(3):171–87.
- 520 Huerta-Cepas, Jaime, Kristoffer Forslund, Luis Pedro Coelho, Damian Szklarczyk, Lars Juhl Jensen,
521 Christian Von Mering, and Peer Bork. 2017. "Fast Genome-Wide Functional Annotation through
522 Orthology Assignment by EggNOG-Mapper." *Molecular Biology and Evolution*.
- 523 Huerta-Cepas, Jaime, Damian Szklarczyk, Kristoffer Forslund, Helen Cook, Davide Heller, Mathias C.
524 Walter, Thomas Rattei, Daniel R. Mende, Shinichi Sunagawa, Michael Kuhn, Lars Juhl Jensen,
525 Christian Von Mering, and Peer Bork. 2016. "EGGNOG 4.5: A Hierarchical Orthology Framework
526 with Improved Functional Annotations for Eukaryotic, Prokaryotic and Viral Sequences." *Nucleic Acids*
527 *Research*.
- 528 Jacobson, Matthew P., David L. Pincus, Chaya S. Rapp, Tyler J. F. Day, Barry Honig, David E. Shaw, and
529 Richard A. Friesner. 2004. "A Hierarchical Approach to All-Atom Protein Loop Prediction." *Proteins:*
530 *Structure, Function and Genetics*.
- 531 Jain, M. R., S. S. Zinjarde, D. D. Deobagkar, and D. N. Deobagkar. 2004. "2,4,6-Trinitrotoluene
532 Transformation by a Tropical Marine Yeast, *Yarrowia Lipolytica* NCIM 3589." *Marine Pollution*
533 *Bulletin* 49(9–10):783–88.
- 534 Jordan, Armin. 2003. "Volcanic Formation of Halogenated Organic Compounds." Pp. 121–39 in *Natural*
535 *Production of Organohalogen Compounds. Handbook of Environmental Chemistry*. Vol. 3, edited by
536 Gribble G. Springer, Berlin, Heidelberg.
- 537 Jung, Jaejoon, Hyoju Seo, Se Hee Lee, Che Ok Jeon, and Woojun Park. 2013. "The Effect of Toxic Malachite

- 538 Green on the Bacterial Community in Antarctic Soil and the Physiology of Malachite Green-Degrading
539 *Pseudomonas* Sp. MGO.” *Applied Microbiology and Biotechnology* 97(10):4511–21.
- 540 Kahlon, Rachhpal S. 2016. “Pseudomonas: Genome and Comparative Genomics.” Pp. 127–91 in
541 *Pseudomonas: Molecular and Applied Biology*, edited by R. S. Kahlon. Cham: Springer International
542 Publishing.
- 543 Kanehisa, Minoru, Yoko Sato, and Kane Morishima. 2016. “BlastKOALA and GhostKOALA: KEGG Tools
544 for Functional Characterization of Genome and Metagenome Sequences.” *Journal of Molecular
545 Biology*.
- 546 Khan, Muhammad Imran, Jaejin Lee, and Joonhong Park. 2013. “A Toxicological Review on Potential
547 Microbial Degradation Intermediates of 2,4,6-Trinitrotoluene, and Its Implications in Bioremediation.”
548 *KSCE Journal of Civil Engineering* 17(6):1223–31.
- 549 Khan, Zeenat, Kunal Jain, Ankita Soni, and Datta Madamwar. 2014. “Microaerophilic Degradation of
550 Sulphonated Azo Dye - Reactive Red 195 by Bacterial Consortium AR1 through Co-Metabolism.”
551 *International Biodeterioration and Biodegradation* 94:167–75.
- 552 Kim, H. Y. and H. G. Song. 2003. “Transformation and Mineralization of 2,4,6-Trinitrotoluene by the White
553 Rot Fungus *Irpex Lacteus*.” *Applied Microbiology and Biotechnology* 61(2):150–56.
- 554 Kim, Hyoun Young, George N. Bennett, and Hong G. Song. 2002. “Degradation of 2,4,6-Trinitrotoluene by
555 *Klebsiella* Sp. Isolated from Activated Sludge.” *Biotechnology Letters* 24(23):2023–28.
- 556 Kitagawa, W., S. Takami, K. Miyauchi, E. Masai, Y. Kamagata, J. M. Tiedje, and M. Fukuda. 2002. “Novel
557 2,4-Dichlorophenoxyacetic Acid Degradation Genes from Oligotrophic *Bradyrhizobium* Sp. Strain
558 HW13 Isolated from a Pristine Environment.” *Journal of Bacteriology* 184(2):509–18.
- 559 Kontro, Jussi, Festus Anasonye, Erika Winquist, Galina Vasilyeva, Kari T. Steffen, and Marja Tuomela.
560 2015. “Bioremediation of TNT Contaminated Soil with Fungi under Laboratory and Pilot Scale
561 Conditions.” *International Biodeterioration & Biodegradation* 105:7–12.
- 562 Kumar, Sudhir, Glen Stecher, and Koichiro Tamura. 2016. “MEGA7: Molecular Evolutionary Genetics
563 Analysis Version 7.0 for Bigger Datasets.” *Molecular Biology and Evolution* 33(7):1870–74.
- 564 Kwak, Young Hak, Dong Seok Lee, and Han Bok Kim. 2003. “*Vibrio Harveyi* Nitroreductase Is Also a
565 Chromate Reductase.” *Applied and Environmental Microbiology* 69(8):4390–95.
- 566 Lee, Bheong Uk, Yun Seok Cho, Sung Chul Park, and Kye Heon Oh. 2009. “Enhanced Degradation of TNT
567 by Genome-Shuffled *Stenotrophomonas Maltophilia* OK-5.” *Current Microbiology* 59(3):346–51.

- 568 Lee, Tai Sung, David S. Cerutti, Dan Mermelstein, Charles Lin, Scott Legrand, Timothy J. Giese, Adrian
569 Roitberg, David A. Case, Ross C. Walker, and Darrin M. York. 2018. "GPU-Accelerated Molecular
570 Dynamics and Free Energy Methods in Amber18: Performance Enhancements and New Features."
571 *Journal of Chemical Information and Modeling* 58(10):2043–50.
- 572 Liang, Shih Hsiung, Duen Wei Hsu, Chia Ying Lin, Chih Ming Kao, Da Ji Huang, Chih Ching Chien, Ssu
573 Ching Chen, Isheng Jason Tsai, and Chien Cheng Chen. 2017. "Enhancement of Microbial 2,4,6-
574 Trinitrotoluene Transformation with Increased Toxicity by Exogenous Nutrient Amendment."
575 *Ecotoxicology and Environmental Safety* 138:39–46.
- 576 Maksimova, Yu. G., A. Yu. Maksimov, and V. A. Demakov. 2018. "Biotechnological Approaches to the
577 Bioremediation of an Environment Polluted with Trinitrotoluene." *Applied Biochemistry and*
578 *Microbiology* 54(8):767–79.
- 579 Márquez, Sebastian L. and Jenny M. Blamey. 2019. "Isolation and Partial Characterization of a New
580 Moderate Thermophilic *Albidovulum* Sp. SLM16 with Transaminase Activity from Deception Island,
581 Antarctica." *Biological Research* 52(1):5.
- 582 Martin, J. L., S. D. Comfort, P. J. Shea, R. A. Drijber, and T. A. Kokjohn. 1997. "Denitration of 2,4,6-
583 Trinitrotoluene by *Pseudomonas Savastanoi*." *Canadian Journal of Microbiology* 43(5):447–55.
- 584 Mercimek, H. A., S. Dincer, G. Guzeldag, A. Ozsavli, and F. Matyar. 2013. "Aerobic Biodegradation of
585 2,4,6-Trinitrotoluene (TNT) by *Bacillus Cereus* Isolated from Contaminated Soil." *Microbial Ecology*
586 66(3):512–21.
- 587 Mercimek, Hatice Aysun, Sadik Dincer, Gulcihan Guzeldag, Aysenur Ozsavli, Fatih Matyar, Afet Arkut,
588 Fikret Kayis, and Melis Sumengen Ozdenefe. 2015. "Degradation of 2,4,6-Trinitrotoluene by *P.*
589 *Aeruginosa* and Characterization of Some Metabolites." *Brazilian Journal of Microbiology* 46(1):103–
590 11.
- 591 Muter, Olga, Katrina Potapova, Baiba Limane, Kristine Sproge, Ida Jakobsone, Guntis Cepurnieks, and
592 Vadims Bartkevics. 2012. "The Role of Nutrients in the Biodegradation of 2,4,6-Trinitrotoluene in
593 Liquid and Soil." *Journal of Environmental Management* 98(1):51–55.
- 594 Oh, B. T., G. Sarath, and P. J. Shea. 2001. "TNT Nitroreductase from a *Pseudomonas Aeruginosa* Strain
595 Isolated from TNT-Contaminated Soil." *Soil Biology and Biochemistry* 33(7–8):875–81.
- 596 Oh, B. T., G. Sarath, P. J. Shea, R. A. Drijber, and S. D. Comfort. 2000. "Rapid Spectrophotometric
597 Determination of 2,4,6-Trinitrotoluene in a *Pseudomonas* Enzyme Assay." *Journal of Microbiological*

- 598 *Methods* 42:149–58.
- 599 Oh, B. T., P. J. Shea, R. A. Drijber, G. K. Vasilyeva, and G. Sarath. 2003. “TNT Biotransformation and
600 Detoxification by a *Pseudomonas Aeruginosa* Strain.” *Biodegradation* 14(5):309–19.
- 601 Pak, J. W., K. L. Knoke, D. R. Noguera, B. G. Fox, and G. H. Chambliss. 2000. “Transformation of 2,4,6-
602 Trinitrotoluene by Purified Xenobiotic Reductase B from *Pseudomonas Fluorescens* I-C.” *Applied and*
603 *Environmental Microbiology* 66(11):4742–50.
- 604 Pereira, W. E., C. E. Rostad, and H. E. Taylor. 1980. “Mount St. Helens, Washington, 1980 Volcanic
605 Eruption: Characterization of Organic Compounds in Ash Samples.” *Geophysical Research Letters*
606 7(11):953–54.
- 607 Reasoner, D. J. and E. E. Geldreich. 1985. “A New Medium for the Enumeration and Subculture of Bacteria
608 from Potable Water.” *Applied and Environmental Microbiology* 49(1):1–7.
- 609 Rieger, Paul Gerhard, Helmut Martin Meier, Michael Gerle, Uwe Vogt, Torsten Groth, and Hans Joachim
610 Knackmuss. 2002. “Xenobiotics in the Environment: Present and Future Strategies to Obviate the
611 Problem of Biological Persistence.” *Journal of Biotechnology* 94(1):101–23.
- 612 Roldán, María Dolores, Eva Pérez-Reinado, Francisco Castillo, and Conrado Moreno-Vivián. 2008.
613 “Reduction of Polynitroaromatic Compounds: The Bacterial Nitroreductases.” *FEMS Microbiology*
614 *Reviews* 32(3):474–500.
- 615 Sabbioni, Gabriele, Yu Ying Liu, Huifang Yan, and Ovnair Sepai. 2005. “Hemoglobin Adducts, Urinary
616 Metabolites and Health Effects in 2,4,6-Trinitrotoluene Exposed Workers.” *Carcinogenesis*
617 26(7):1272–79.
- 618 Seemann, Torsten. 2014. “Prokka: Rapid Prokaryotic Genome Annotation.” *Bioinformatics*.
- 619 Serrano-González, Mónica Y., Rashmi Chandra, Carlos Castillo-Zacarias, Felipe Robledo-Padilla, Magdalena
620 de J. Rostro-Alanis, and Roberto Parra-Saldivar. 2018. “Biotransformation and Degradation of 2,4,6-
621 Trinitrotoluene by Microbial Metabolism and Their Interaction.” *Defence Technology* 14(2):151–64.
- 622 Sievers, Fabian and Desmond G. Higgins. 2014. “Clustal Omega.” *Current Protocols in Bioinformatics*.
- 623 Singh, Baljinder, Jagdeep Kaur, and Kashmir Singh. 2012. “Microbial Remediation of Explosive Waste.”
624 *Critical Reviews in Microbiology* 38(2):152–67.
- 625 Stenuit, Ben A. and Spiros N. Agathos. 2010. “Microbial 2,4,6-Trinitrotoluene Degradation: Could We Learn
626 from (Bio)Chemistry for Bioremediation and Vice Versa?” *Applied Microbiology and Biotechnology*
627 88(5):1043–64.

- 628 Tam, Le Thi, Christine Eymann, Dirk Albrecht, Rabea Sietmann, Frieder Schauer, Michael Hecker, and
629 Haike Antelmann. 2006. "Differential Gene Expression in Response to Phenol and Catechol Reveals
630 Different Metabolic Activities for the Degradation of Aromatic Compounds in *Bacillus Subtilis*."
631 *Environmental Microbiology* 8(8):1408–27.
- 632 Thijs, S., W. Sillen, S. Truyens, B. Beckers, J. van Hamme, P. van Dillewijn, P. Samyn, R. Carleer, N.
633 Weyens, and Jaco Vangronsveld. 2018. "The Sycamore Maple Bacterial Culture Collection From a
634 TNT Polluted Site Shows Novel Plant-Growth Promoting and Explosives Degrading Bacteria."
635 *Frontiers in Plant Science* 9:1134.
- 636 Toogood, Helen S., John M. Gardiner, and Nigel S. Scrutton. 2010. "Biocatalytic Reductions and Chemical
637 Versatility of the Old Yellow Enzyme Family of Flavoprotein Oxidoreductases." *ChemCatChem*
638 2(8):892–914.
- 639 Tralau, Tewes, Eun Chan Yang, Carola Tralau, Alasdair M. Cook, and Frithjof C. Küpper. 2011. "Why Two
640 Are Not Enough: Degradation of *p*-Toluenesulfonate by a Bacterial Community from a Pristine Site in
641 Moorea, French Polynesia." *FEMS Microbiology Letters* 316(2):123–29.
- 642 Vorbeck, Claudia, Hiltrud Lenke, Peter Fischer, Jim C. Spain, and Hans Joachim Knackmuss. 1998. "Initial
643 Reductive Reactions in Aerobic Microbial Metabolism of 2,4,6- Trinitrotoluene." *Applied and*
644 *Environmental Microbiology* 64(1):246–52.
- 645 Waterhouse, Andrew, Martino Bertoni, Stefan Bienert, Gabriel Studer, Gerardo Tauriello, Rafal Gumienny,
646 Florian T. Heer, Tjaart A. P. De Beer, Christine Rempfer, Lorenza Bordoli, Rosalba Lepore, and
647 Torsten Schwede. 2018. "SWISS-MODEL: Homology Modelling of Protein Structures and
648 Complexes." *Nucleic Acids Research*.
- 649 Wawrik, Boris, Lee Kerkhof, Gerben J. Zylstra, and Jerome J. Kukor. 2005. "Identification of Unique Type II
650 Polyketide Synthase Genes in Soil." *Applied and Environmental Microbiology* 71(5):2232–38.
- 651 Williams, Richard E., Deborah A. Rathbone, Nigel S. Scrutton, and Neil C. Bruce. 2004. "Biotransformation
652 of Explosives by the Old Yellow Enzyme Family of Flavoproteins." *Applied and Environmental*
653 *Microbiology* 70(6):3566–74.
- 654 Winsor, Geoffrey L., Thea Van Rossum, Raymond Lo, Bhavjinder Khaira, Matthew D. Whiteside, Robert E.
655 W. Hancock, and Fiona S. L. Brinkman. 2009. "*Pseudomonas* Genome Database: Facilitating User-
656 Friendly, Comprehensive Comparisons of Microbial Genomes." *Nucleic Acids Research*.
- 657 Wittich, Rolf Michael, Alí Haïdour, Pieter Van Dillewijn, and Juan Luis Ramos. 2008. "OYE Flavoprotein

658 Reductases Initiate the Condensation of TNT-Derived Intermediates to Secondary Diarylamines and
659 Nitrite." *Environmental Science and Technology* 42(3):734–39.

660 Won, W. D., L. H. DiSalvo, and J. Ng. 1976. "Toxicity and Mutagenicity of 2,4,6 Trinitrotoluene and Its
661 Microbial Metabolites." *Applied and Environmental Microbiology* 31(4):576–580.

662

663

664

665

666

667

668

669

670

671

672

673

674

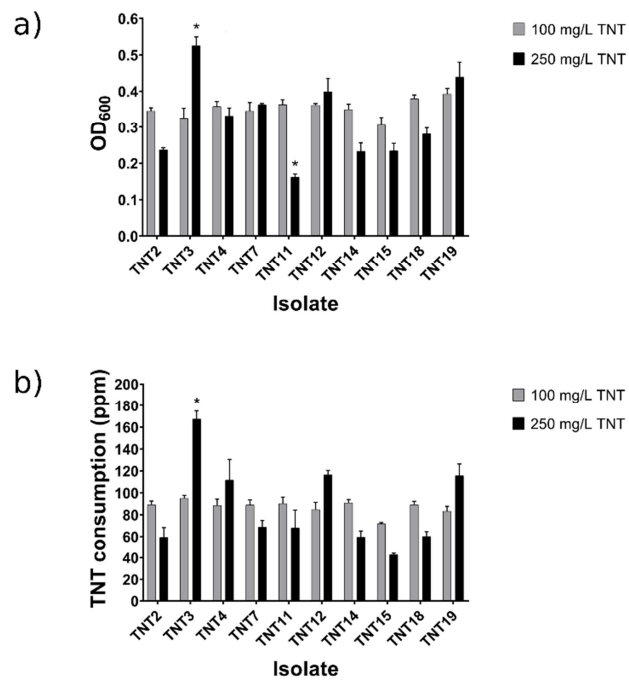
675

676

677

678

679



680

681

682 **Figure 1. Growth and TNT consumption of *Pseudomonas* isolates from Antarctic soil samples.** a) Growth of the
 683 isolates at 100 mg/L (gray bars) and 250 mg/L TNT (black bars). b) TNT consumption by the isolates at 100 mg/L (gray
 684 bars) and 250 mg/L TNT (black bars). The cultures were incubated for 6 days at 21°C. Data are reported as the
 685 average \pm standard deviation of five independent experiments. Asterisks (*) indicate a statistically significant difference (p
 686 < 0.05).

687

688

689

690

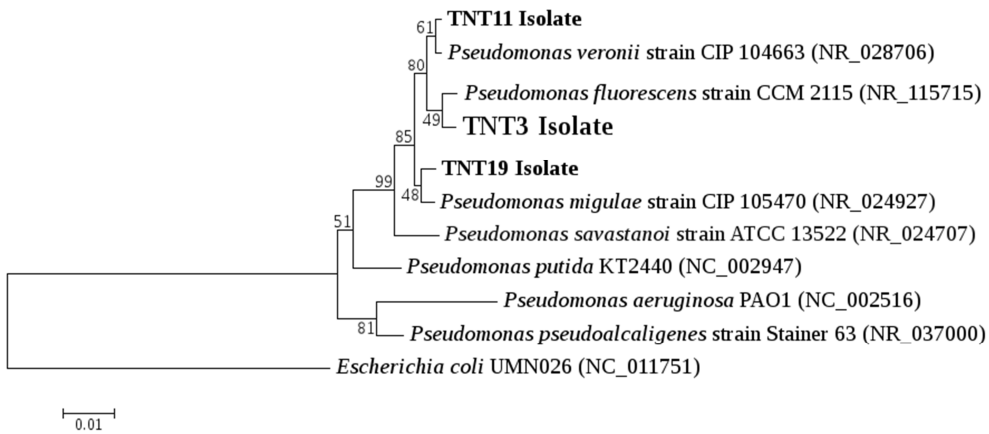
691

692

693

694

695



696

697

698 **Figure 2. Phylogenetic tree of the selected isolates.** Phylogenetic tree based on complete 16S rRNA gene sequences
 699 showing the position of three isolates (TNT3, TNT11, and TNT19) among related taxa within the genus *Pseudomonas*. The
 700 phylogenetic tree was constructed using the Neighbor-Joining (NJ) method with 1000 bootstrap replicates. *Escherichia coli*
 701 UMN026 was used as outgroup. GenBank accession numbers are shown in parentheses.

702

703

704

705

706

707

708

709

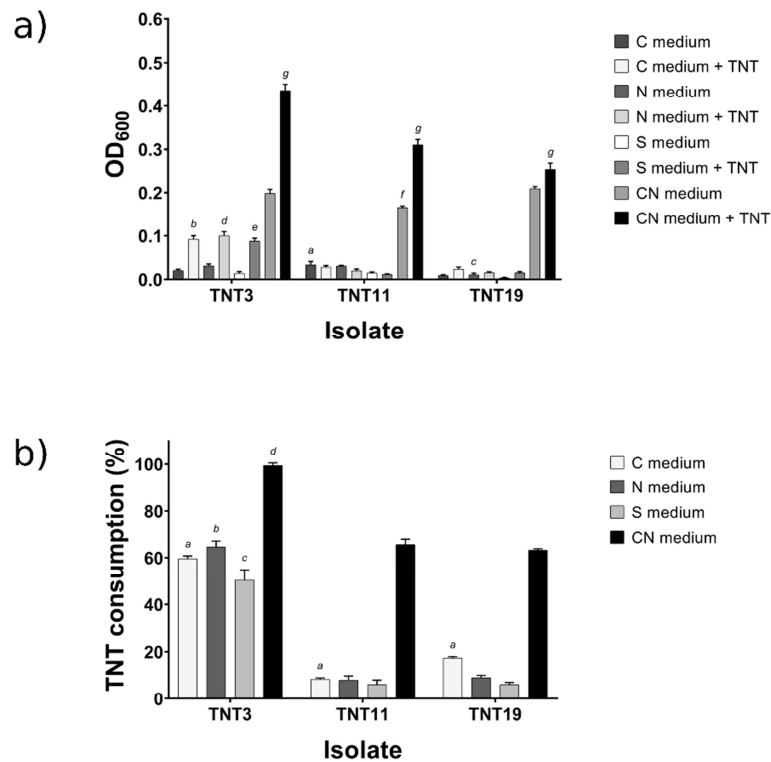
710

711

712

713

714



715

716 **Figure 3. Growth and TNT consumption of the selected isolates in different culture media.** a) Growth of the isolates in
 717 C (saline M9 medium containing 0.8% glucose), N (saline M9 medium containing 0.05% NH₄Cl), S (saline medium M9),
 718 and CN medium (half-diluted R2A medium) without and with TNT (100 mg/L). b) TNT consumption (%) by the isolates in
 719 the same media mentioned above. 100% corresponds to 100 ppm TNT. The cultures were incubated for 6 days at 28°C.
 720 Data are reported as the average \pm standard deviation of four independent experiments. Italic letters indicate a statistically
 721 significant difference ($p < 0.05$).

722

723

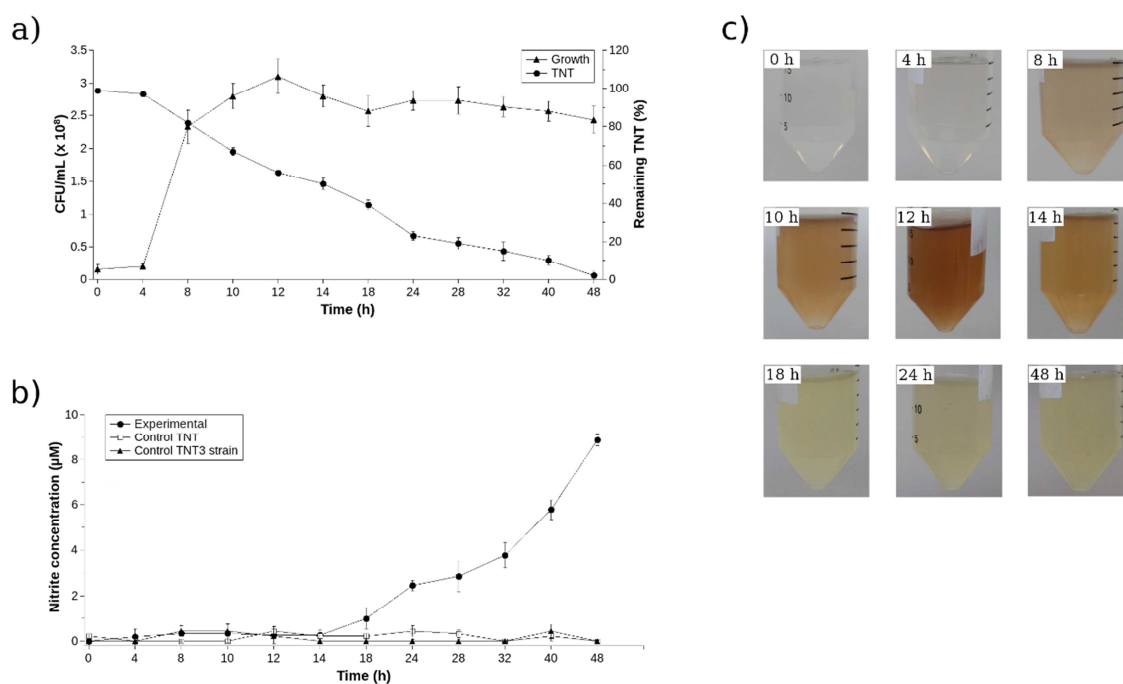
724

725

726

727

728



729

730

731 **Figure 4. Growth curve and TNT biodegradation by *Pseudomonas* sp. TNT3.** a) The bacterium was grown in CN
 732 medium containing 100 mg/L TNT (100%). Time course of the bacterial growth expressed as CFU/mL (triangles) and the
 733 remaining TNT expressed as percentage (circles). Data are reported as the average \pm standard deviation of three
 734 independent experiments. b) Accumulation of nitrite during TNT consumption by strain TNT3 (experimental, closed
 735 circles), control TNT (open squares), and control strain TNT3 without TNT (closed triangles). Data are reported as the
 736 average \pm standard deviation of three independent experiments. c) Color change of culture medium during bacterial growth
 737 in presence of TNT at different time intervals.

738

739

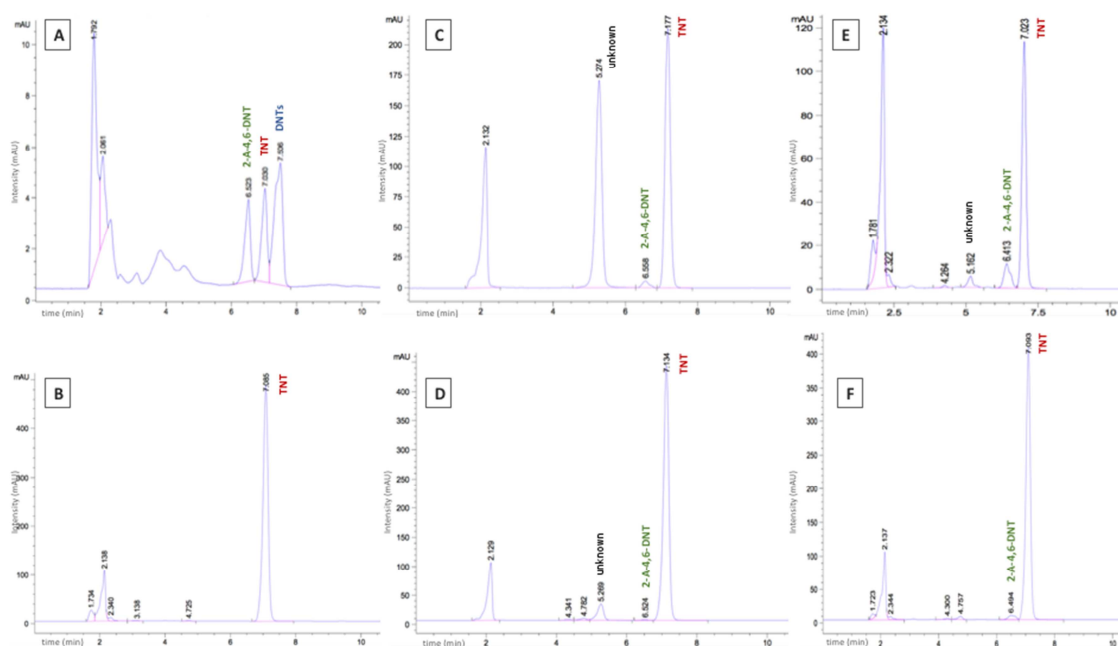
740

741

742

743

744



745

746

747 **Figure 5. High-performance liquid chromatography chromatograms for TNT biotransformation by *Pseudomonas***

748 **sp. TNT3 and *P. putida* KT2440.** a) Chromatograms of the standard mixture (1 mg/L each one). b) Initial TNT

749 concentration (100 mg/L). c) and d) Supernatants of strain TNT3 and strain KT2440 cultures after incubating for 12 h at

750 28°C, respectively. e) and f) Supernatants of strain TNT3 and strain KT2440 cultures after incubating for 48 h at 28°C,

751 respectively. A representative chromatogram of the triplicates is shown for each condition. TNT= trinitrotoluene; 2-A-4,6-

752 DNT= 2-amino-4,6-dinitrotoluene; DNTs= 2,4-dinitrotoluene and 2,6-dinitrotoluene.

753

754

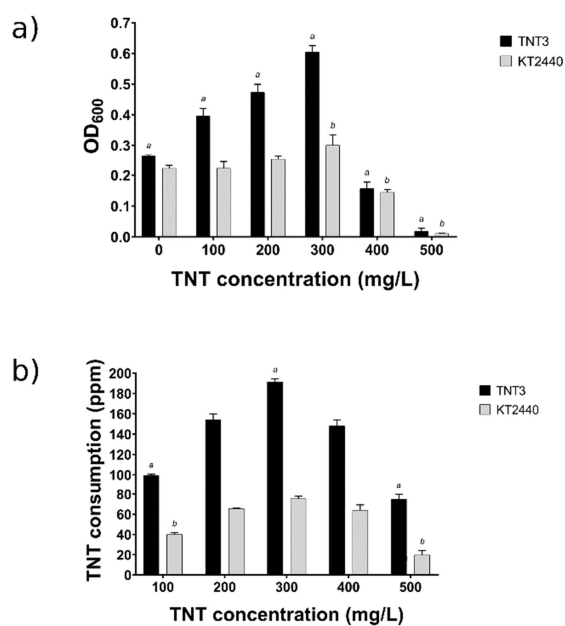
755

756

757

758

759



760

761

762 **Figure 6. Growth and TNT consumption by *Pseudomonas* sp. TNT3 and *P. putida* KT2440 at different TNT**
 763 **concentrations.** a) Growth (OD₆₀₀) of strain TNT3 (black bars) and strain KT2440 (gray bars) at different concentrations
 764 of TNT. b) TNT consumption (ppm) by strain TNT3 (black bars) and strain KT2440 (gray bars) at different concentrations
 765 of TNT. The cultures were incubated for 2 days at 28°C. Data are reported as the average \pm standard deviation of three
 766 independent experiments. Italic letters indicate a statistically significant difference ($p < 0.05$).

767

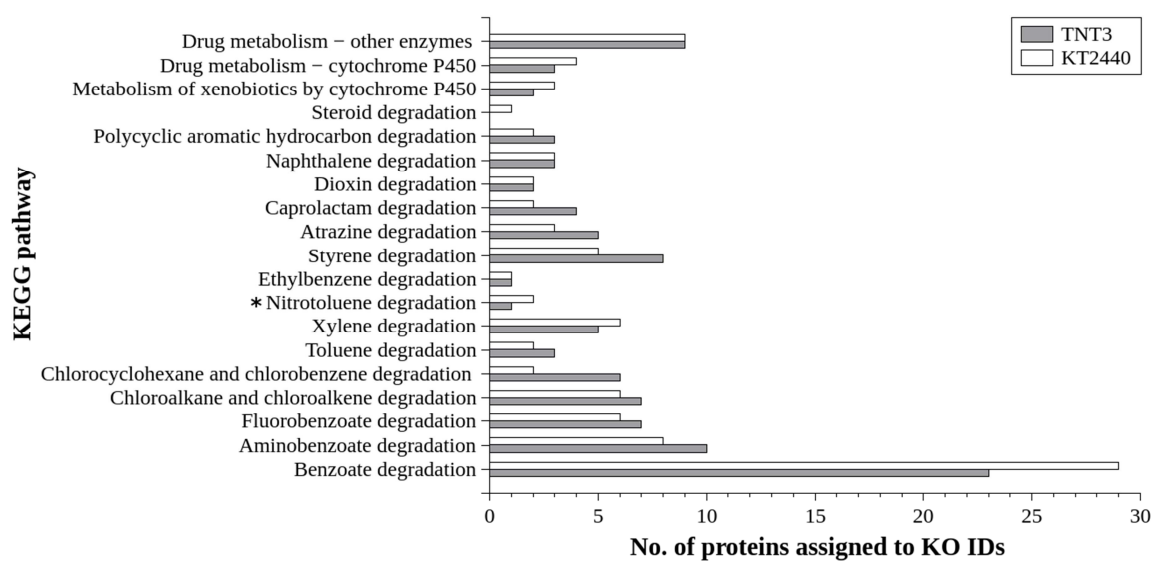
768

769

770

771

772



773

774

775 **Figure 7. Comparison of xenobiotic biodegradation KEGG pathways between *Pseudomonas* sp. TNT3 and *P. putida***

776 **KT2440.** The axis-x corresponds to the number of the KO IDs (ortholog groups) found in the functional annotation of each

777 genome for each pathway. Results were obtained using BlastKOALA, except for the TNT3 ortholog in the Nitrotoluene

778 degradation pathway (*) found with egg-NOG.

779

780

781

782

783

784

785

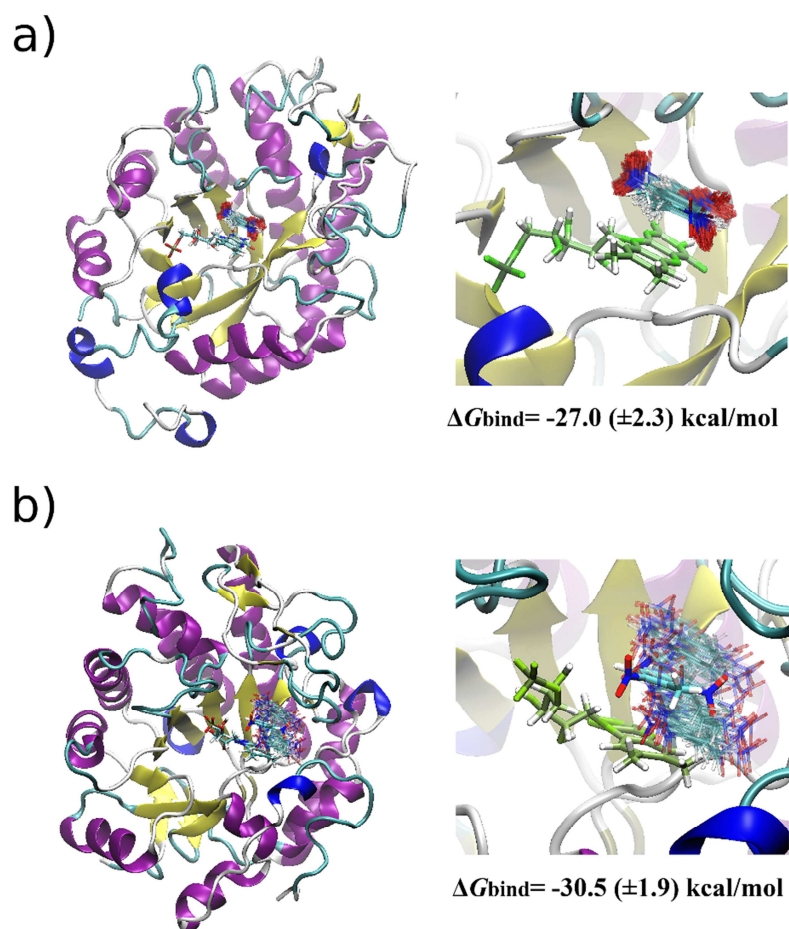
786

787

788

789

790



791

792

793 **Figure 8. Representation of the enzyme-ligand complex after 300 ns of molecular dynamics for a) Xena_TNT3 and**

794 **b) XenB_TNT3.** Overall representation of each simulated system is shown on the left. Zoom-in of the catalytic sites are

795 shown on the right. For each system, the superimposition of 30 conformations adopted by the ligand TNT (cyan) near the

796 cofactor FMN (green) every 10 ns is shown. The ligand binding energies shown in the figure were calculated using the

797 MMGBSA method considering the last 100 ns of dynamics.

798

799

800

801

802

803 **Table 1.** Functional annotation results for the 7 sequences of *Pseudomonas* sp. TNT3 identified by HMM and BLAST
 804 homology search as candidates for TNT degradation activity.

805

Sequence	PROKKA	Eggnog			KEGG
	Annotation	Ortholog	Organism	KO	Pathway
CDS_03039	<i>N</i> -ethylmaleimide reductase*	PFWH6_1400 (XENB)	<i>P. fluorescens</i> WH6	K10680	ko00633
CDS_02682	NADPH dehydrogenase*	PFL_1121 (XENA)	<i>P. fluorescens</i> Pf-5	K00354	Unclassified
CDS_03801	NADH oxidase	PFL01_0884	<i>P. fluorescens</i> Pf0-1	NA	NA
CDS_01069	Putative NAD(P)H nitroreductase YdjA	PFL01_1480 (YDJA)	<i>P. fluorescens</i> Pf0-1	NA	NA
CDS_00209	5,6-dimethylbenzimidazole synthase	Pfl01_1643 (BLUB)	<i>P. fluorescens</i> Pf0-1	K00768	ko00860
CDS_00327	putative N-methylproline demethylase	PSF113_5447 (DGCA)	<i>P. fluorescens</i> F113	K00219	Unclassified
CDS_01856	2,4-dienoyl-CoA reductase A	PSF113_3907	<i>P. fluorescens</i> F113	K00219	Unclassified

806

807 Annotations were performed using egg-NOG, BlastKOALA and PROKKA. Sequences only identified by BLAST
 808 homology search (*). NA Not Assigned.

809

810

Highlights

- A new TNT transforming strain *Pseudomonas* sp. TNT3 was isolated from Antarctica.
- *Pseudomonas* sp. TNT3 completely transforms 100 ppm TNT after 48 h at 28°C.
- The *Pseudomonas* sp. TNT3 genome was sequenced and functionally annotated.
- TNT-degrading enzymes were identified in the genome and studied *in silico*.

Declarations of interest

All authors declare no conflicts of interest.

Journal Pre-proof